Commun. Theor. Phys. (Beijing, China) **43** (2005) pp. 765–768

Vol. 43, No. 4, April 15, 2005

Theory of Electrorotation of Clustered Colloidal Particles

LIU Ren-Ming[1] and HUANG Ji-Ping[2,3,*]

[1]Department of Physics, Huaiyin Teachers College, Huaiyin 223001, China

[2]Department of Physics, the Chinese University of Hong Kong, Shatin, NT, Hong Kong, China

[3]Max Planck Institute for Polymer Research, Ackermannweg 10, 55128, Mainz, Germany

(Received September 8, 2004)

Abstract *When a colloidal suspension is exposed to a strong rotating electric field, an aggregation of the suspended particles is induced to appear. In such clusters, the separation between the suspended particles is so close that one could not neglect the multiple image effect on the electrorotation (ER) spectrum. Since so far the exact multiple image method exists in two dimensions only, rather than in three dimensions, we investigate the ER spectrum of the clustered colloidal particles in two dimensions, in which many cylindrical particles are randomly distributed in a sheet cluster. We report the dependence of the ER spectrum on the material parameters. It is shown that the multiple image method predicts two characteristic frequencies, at which the rotation speed reaches maximum. To this end, the multiple image method is numerically demonstrated to be in good agreement with the known Maxwell–Garnett approximation.*

PACS numbers: 82.70.Dd, 77.22.Ej, 77.84.Nh
Key words: electrorotation, colloidal particles

1 Introduction

By using dielectrophoresis[1] and electrorotation (ER),[2] one may monitor the dielectric properties of dispersions of colloids or biological cells. It is important to study their frequency-dependent responses to ac electric fields, which yields valuable information on the structural (Maxwell–Wagner) polarization effects.[3,4] The polarization is characterized by a variety of characteristic frequency-dependent changes known as the dielectric dispersion. In particular, for the β-dispersion (also called the Maxwell–Wagner dispersion, ranging from kHz to MHz), it suffices to focus on the induced dipole moments of the particles.

In the last two decades, various experimental tools have been developed to analyze the polarization of biological cells, such as dielectric spectroscopy,[5] dielectrophoresis,[6] and electrorotation techniques.[7] Among these techniques, conventional dielectrophoresis and electrorotation are usually applied to analyze the frequency dependence of translations and rotations of individual cells in an inhomogeneous and rotating electric field, respectively.[6,7] Furthermore, one is able to monitor the cell movements by using automated video analysis[8] as well as light scattering methods.[4] Actually, ER is caused by the existence of a phase difference between the field-induced dipole moment and the external rotating field, which results in a desired torque.

In the dilute limit, the ER of individual particle can be predicted by ignoring the mutual interaction between the cells, and hence may be considered as isolated particle in rotation (e.g., Ref. [9], and references therein). However, the cells may aggregate under the influence of the external field. In this case the Brownian motion can be neglected, and the cell system becomes non-dilute even though it is initially dilute. In order to discuss the ER spectrum for low concentration case, we applied Maxwell–Garnett approximation (MGA),[10] which takes into account the local field effect.[11,12] Actually, when a colloidal suspension is exposed to a strong rotating electric field, an aggregation of the suspended particles will appear. As a result, clustering behavior is often seen. Since the particle concentration in the cluster is high, the particles are hence quite close to each other. In such sheet clusters, the effect of multiple images arising from all the other particles should be important accordingly. In this regard, the multiple image effect should be taken into account when we investigate the corresponding ER spectrum. As an initial model, we have recently studied the ER of two approaching spherical particles in the presence of a rotating electric field.[13] We showed that when the two particles approach and finally touch, the mutual polarization interaction between the particles leads to a change in the dipole moment of individual particles and hence the ER spectrum, as compared to that of isolated particles, via the multiple image method.[14]

Accordingly, in the present work we shall discuss the ER spectrum of clusters by including the multiple image effect arising from all the other particles. Fortunately, one examined the case of circular inclusions in a conducting sheet (two-dimensional), and the two-inclusion problem was solved exactly by using the method of multiple images.[15] In this work, we shall discuss a two-dimensional case, in which many cylindrical particles are randomly distributed in a sheet cluster.

2 Formalism

Let us start by considering the circular cylindrical particles of complex dielectric constant $\tilde{\epsilon}_1 = \epsilon_1 + \sigma_1/\mathrm{i}2\pi f$

*E-mail: jphuang@mpip-mainz.mpg.de

with concentration p, randomly embedded in a sheet. The complex dielectric constant of the surrounding medium is $\tilde{\epsilon}_2 = \epsilon_2 + \sigma_2/\mathrm{i}2\pi f$ with f being the frequency of the external electric field and $\mathrm{i} = \sqrt{-1}$. Here ϵ and σ are respectively the real dielectric constant and conductivity.

In view of the proportional dependence of the electroroation velocity on the imaginary part[2] of the dipole factor (also called Clausius–Mossotti factor), we shall numerically discuss the imaginary part of the dipole factor instead in the following. In this regard, we shall first determine the dipole factor of a specific particle.

It is known that the dipole factor of an isolated particle has the following general form

$$b = \frac{n(\tilde{\epsilon}_1 - \tilde{\epsilon}_2)}{\tilde{\epsilon}_2 + n(\tilde{\epsilon}_1 - \tilde{\epsilon}_2)} \tag{1}$$

with n being the depolarizing factor. In the present paper, perpendicular to the symmetry axis of an isolated cylinder (in two dimensions) $n = 1/2$, this general form is naturally reduced to

$$b = \frac{\tilde{\epsilon}_1 - \tilde{\epsilon}_2}{\tilde{\epsilon}_1 + \tilde{\epsilon}_2}\,. \tag{2}$$

The spectral representation approach[16,17] offers a method for separating the material parameters (e.g., dielectric constant and conductivity) from the structure geometrical parameters in a rigorous manner, thus simplifying the investigation. In order to introduce the spectral representation, we define two material parameters as

$$s = \left(1 - \frac{\epsilon_1}{\epsilon_2}\right)^{-1} \quad \text{and} \quad t = \left(1 - \frac{\sigma_1}{\sigma_2}\right)^{-1}. \tag{3}$$

They are both functions of the conductivity ratio and real dielectric constant ratio, respectively. After some manipulation, we obtain

$$b = \frac{F_1}{s - s_1} + \frac{\delta\epsilon_1}{1 + \mathrm{i}\, f/f_c} \tag{4}$$

with two geometrical parameters $F_1 = -1/2$ and $s_1 = 1/2$, where the dispersion strength and the characteristic frequency are respectively given by

$$\delta\epsilon_1 = F_1 \frac{s - t}{(t - s_1)(s - s_1)}\,,$$

$$f_c = \frac{1}{2\pi}\frac{\sigma_2}{\epsilon_2}\frac{s(t - s_1)}{t(s - s_1)}\,. \tag{5}$$

Thus, there is only one characteristic frequency in the ER spectrum of an isolated particle, at which the rotational speed reaches maximum.

If the suspension contains clustered particles, the multiple image effect should be taken into account. In this case, the effective dielectric constant of the sample to the second order in the concentration p is given by[15]

$$\frac{\tilde{\epsilon}_e}{\tilde{\epsilon}_2} = 1 + 2bp + 2b^2p^2 + b^2p^2F(b)\,. \tag{6}$$

Here $F(b)$ is an odd function of b, which contains the contribution from the dipole moment of all the particles to the effective dielectric constant. And it is determined by[15]

$$F(b) = 16\int_0^\infty \sum_{n=1}^{\infty} b^{2n-1}\frac{\sinh^3\gamma\cosh\gamma}{\sinh^2(2n+1)\gamma}\,\mathrm{d}\gamma \tag{7}$$

with γ satisfying the relation $\cosh\gamma = R/D$, where R represents the center-to-center separation between the particles with diameter D. Here it is worth while noting that this equation has included the effect of all the multiple images inside the system accurately.

Next, to discuss the electrorotation of a special cylindrical particle in the clustered particles, it is straightforward to obtain the dipole factor as

$$b^* = \frac{\tilde{\epsilon}_1 - \tilde{\epsilon}_e}{\tilde{\epsilon}_1 + \tilde{\epsilon}_e}\,. \tag{8}$$

Here we should remark that b^* [Eq. (8)] contains the contribution from all the multiple images within the system under consideration.

Alternatively, the effective dielectric constant $\tilde{\epsilon}'_e$ may be determined by the well-known Maxwell–Garnett approximation (MGA),[10] namely

$$p\frac{\tilde{\epsilon}_1 - \tilde{\epsilon}_2}{\tilde{\epsilon}_1 + \tilde{\epsilon}_2} = \frac{\tilde{\epsilon}'_e - \tilde{\epsilon}_2}{\tilde{\epsilon}'_e + \tilde{\epsilon}_2}\,. \tag{9}$$

in an attempt to include the local-field effect. Then the dipole factor b_{MGA} determined by the MGA is given by

$$b_{\mathrm{MGA}} = \frac{\tilde{\epsilon}_1 - \tilde{\epsilon}'_e}{\tilde{\epsilon}_1 + \tilde{\epsilon}'_e}\,. \tag{10}$$

Again, we should note that b_{MGA} [Eq. (10)] has included all the local-field effect existing in the suspension of interest. Equations (8) and (10) are the main results of the present paper.

3 Numerical Results

We are now in a position to do some numerical calculations. In Figs. 1 and 2, we investigate the multiple image effect on the ER of clusters. To one's interest, two ER characteristic frequencies occur always. More precisely, both the two peaks relate to the co-field rotation only, which are potentially different from those respectively related to co- or anti-field rotations. In fact, in the present theory similar results may also be obtained for the anti-field rotation which can be achieved by altering the material parameters (no figures shown here). In addition, the location of the characteristic frequency for an isolated particle is different from the one predicted by the multiple image method or MGA (see Fig. 3 below). In detail, both the multiple image effect and local-field effect may strongly reduce the peak value predicted for the isolated particle. Also, in contrast to the isolated particle, a red-shift and blue-shift of the characteristic frequency are always shown for the left characteristic frequency and the right, respectively. Here the red-shift (or blue-shift) means that the characteristic frequency is located in a lower (or higher) frequency.

In Fig. 1, it is shown that the conductivity effect (i.e., t and σ_2) plays an important role in the characteristic frequencies. In this case, the red-shift of the characteristic frequency is obtained by changing conductivities. However, the role of the dielectric constant (namely, s and ϵ_2) is minor even though the red-shift is observed as well.

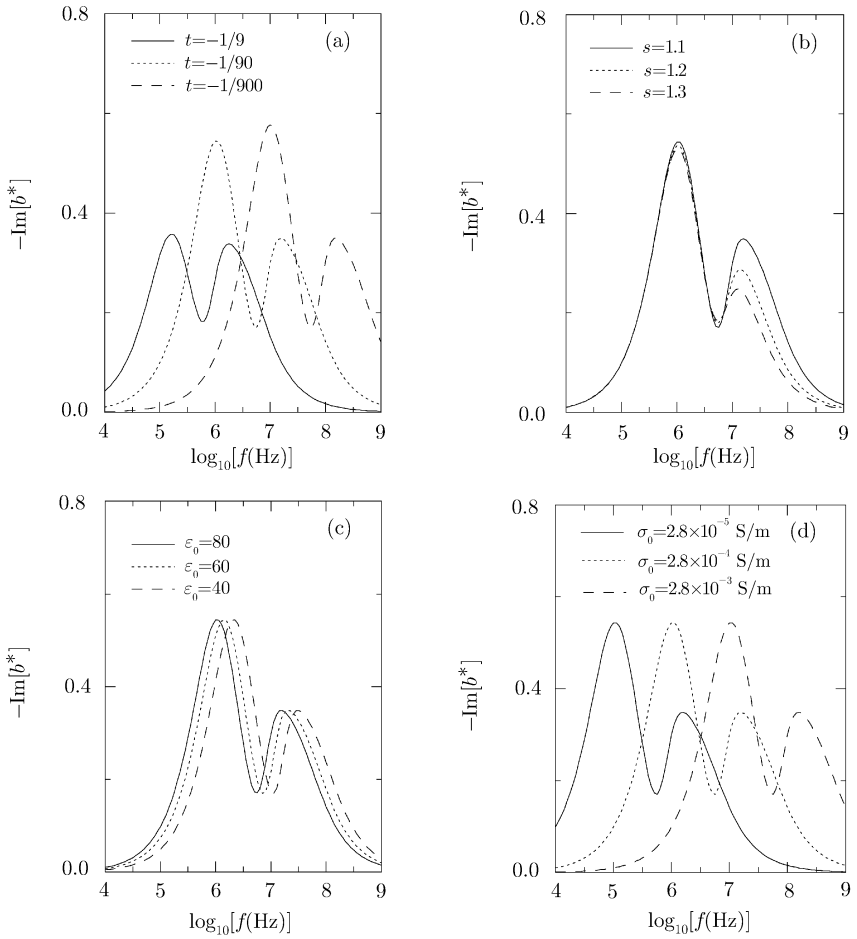

Fig. 1 ER spectrum given by $-\mathrm{Im}[b^*]$ as a function of the frequency for $p = 0.6$ and closest $R/D = 1.01$. Parameters: (a) $s = 1.1$, $\epsilon_2 = 80$, and $\sigma_2 = 2.8 \times 10^{-4}\,\mathrm{S/m}$; (b) $t = -1/90$, $\epsilon_2 = 80$, and $\sigma_2 = 2.8 \times 10^{-4}\,\mathrm{S/m}$; (c) $t = -1/90$, $s = 1.1$, and $\sigma_2 = 2.8 \times 10^{-4}\,\mathrm{S/m}$; (d) $s = 1.1$, $t = -1/90$, and $\epsilon_2 = 80$.

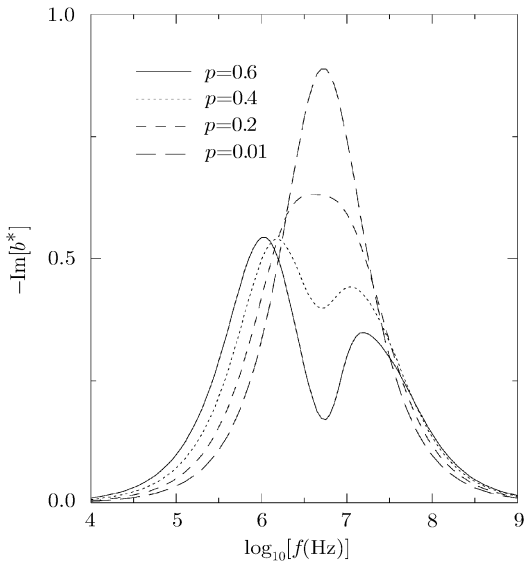

Fig. 2 ER spectrum given by $-\mathrm{Im}[b^*]$ as a function of the frequency for different concentration p. Parameters: $\epsilon_2 = 80$, $\sigma_2 = 2.8 \times 10^{-4}\,\mathrm{S/m}$, $s = 1.1$, and $t = -1/90$.

Figure 2 displays the influence of concentration. We find that the high concentration predicts two characteristic frequencies, whereas the low predicts only one. That is, in the case of high concentration, the multiple image effect does play an important role. Note that $p = 0.01$ here may be approximated as the case of an isolated particle, for which only one characteristic frequency is predicted, as expected.

We investigate three cases in Fig. 3: (i) many cylinders randomly disperse in a cluster by considering the multiple image effect; (ii) the same as (i), but based upon the MGA, namely the local-field effect is considered;[11] (iii) isolated cylinder. Firstly, we compare cases (i) with (ii). We find that the MGA predicts two characteristic frequencies, as also shown in Ref. [11]. Above all, both methods are shown to be in good agreement. When we used the MGA to discuss the ER characteristic frequency in a recent work,[11] two peaks were actually predicted as well, but they are located close enough to be overlapped due to low concentration. In contrast to the present phenomena of two separated ER peaks predicted by the MGA, it is further shown that the local-field effect becomes stronger for increasing concentrations. However, we believe the

present mutiple image method predicts a more exact result. Secondly, we compare cases (i) with (iii). The characteristic frequency obtained from the multiple image effect may red-shift or blue-shift when compared with that for the isolated particle, as mentioned above already. Finally, regarding the comparison between (2) and (3), we refer the reader to Ref. [11].

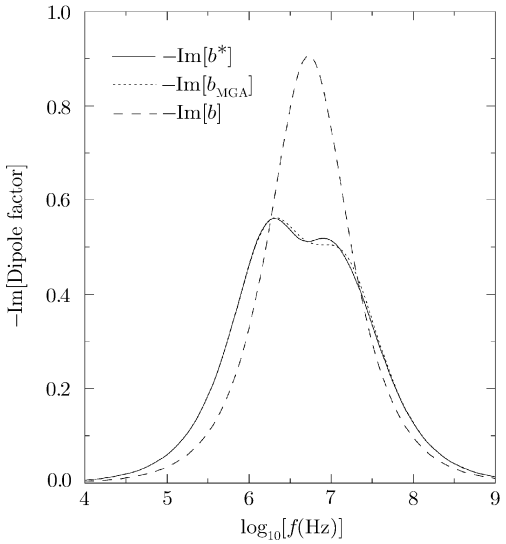

Fig. 3 ER spectrum given by −Im[Dipole factor] as a function of the frequency for three cases: (i) many cylinders randomly distributed in a cluster by considering the multiple image effect (−Im[b^*]); (ii) same as (i), but based on the MGA (−Im[$b_{\rm MGA}$]); (iii) isolated cylinder (−Im[b]). Parameters: $\epsilon_2 = 80$, $\sigma_2 = 2.8 \times 10^{-4}$ S/m, $s = 1.1$, and $t = -1/90$.

4 Discussion and Conclusion

We have considered homogeneous, cylindrical particles in a cluster sheet, which is exposed to a rotating electric field. Within this structure, the concentration of the particles is very high, and hence the separation between the particles is quite small. Therefore, the multiple image arising from all the other particles has to be taken into account. Also, we have compared the results obtained from the MGA and the mutiple image method, respectively, and good agreement between them has been numerically demonstrated. Here, the multiple image method predicts a more exact result than the MGA (an approximate mean-field theory).

It was shown that the multipolar interaction shifts a peak to a lower frequency.[13] But in the current paper we have found that a peak is higher than that of the isolated-particle case, which is actually due to the many-body (local-field) effect arising from the many-particle system under consideration.

We believe our theory is valid for the case of low Reynolds numbers. In the present study, both the radii and the angular velocities of the particles are small. Thus, we have safely applied the MGA and multiple image method, which are both valid when the particles are at rest.

We also realize the appearance of a circular medium flow because all the particles rotate in the same direction. The macroscopic spin rate drives the suspending liquid, leading to a decrease of the apparent viscosity of the suspension,[18] but not affecting the dipole factor. Finally, it is also instructive to extend the present theory to non-spherical[12] and inhomogeneous (e.g. the so-called graded cells[19]) cells, or to the system in which lattice effects[20] play a role.

Acknowledgments

This work was supported by the Alexander von Humboldt Foundation of Germany (J.P.H.). J.P.H. acknowledges professor K.W. Yu's fruitful discussions.

References

[1] H.A. Pohl, *Dielectrophoresis*, Cambridge Univ. Press, Cambridge (1978).
[2] T.B. Jones, *Electromechanics of Particles*, Cambridge Univ. Press, Cambridge (1995).
[3] For a review, see J. Gimsa and D. Wachner, Biophys. J. **77** (1999) 1316.
[4] J. Gimsa, Ann. NY Acad. Sci. **873** (1999) 287.
[5] K. Asami, T. Hanai, and N. Koizumi, Jpn. J. Appl. Phys. **19** (1980) 359.
[6] G. Fuhr, J. Gimsa, and R. Glaser, Stud. Biophys. **108** (1985) 149.
[7] J. Gimsa, P. Marszalek, U. Lowe, and T.Y. Tsong, Biophys. J. **60** (1991) 749.
[8] G. De Gasperis, X.B. Wang, J. Yang, F.F. Becker, and P.R.C. Gascoyne, Meas. Sci. Technol. **9** (1998) 518.
[9] J.P. Huang, K.W. Yu, G.Q. Gu, and M. Karttunen, Phys. Rev. **E67** (2003) 051405; J.P. Huang and K.W. Yu, Commun. Theor. Phys. (Beijing, China) **39** (2003) 506.
[10] J.C.M. Garnett, Philos. Trans. R. Soc. London **203** (1904) 385; ibid **205** (1906) 237.
[11] J.P. Huang, K.W. Yu, and G.Q. Gu, Phys. Lett. **A300** (2002) 385.
[12] L. Gao, J.P. Huang, and K.W. Yu, Phys. Rev. **E67** (2003) 021910.
[13] J.P. Huang, K.W. Yu, and G.Q. Gu, Phys. Rev. **E65** (2002) 021401.
[14] K.W. Yu and Jones T.K. Wan, Comput. Phys. Commun. **129** (2000) 177.
[15] B.R. Djordjevic, J.H. Hetherington, and M.F. Thorpe, Phys. Rev. **B53** (1996) 14862.
[16] D.J. Bergman, Phys. Rep. **43** (1978) 377.
[17] Jun Lei, Jones T.K. Wan, K.W. Yu, and Hong Sun, Phys. Rev. **E64** (2001) 012903.
[18] H. Brenner, Ann. Rev. Fluid Mech. **2** (1970) 137.
[19] J.P. Huang and K.W. Yu, Appl. Phys. Lett. **85** (2004) 94.
[20] J.P. Huang, Phys. Rev. **E70** (2004) 041403; Chem. Phys. Lett. **390** (2004) 380.